

# Interpreting Pump - Probe Experiments on Dimethyl Methyl Phosphonate (DMMP)

**A Thesis**

submitted to

Indian Institute of Science Education and Research Pune  
In partial fulfillment of the requirements for the  
BS-MS Dual Degree Programme

by

Vaibhav Singh



Indian Institute of Science Education and Research Pune  
Dr. Homi Bhabha Road,  
Pashan, Pune 411008, INDIA.

April, 2019

Supervisors: Spiridoula Matsika, Department of Chemistry,  
Temple University, Philadelphia, USA.  
Anirban Hazra, Department of Chemistry, IISER Pune.

© Vaibhav Singh 2019

All rights reserved

# Certificate

This is to certify that this dissertation entitled *Interpreting Pump - Probe Experiments on Dimethyl Methyl Phosphonate (DMMP)* towards the partial fulfillment of the BS-MS dual degree program at the Indian Institute of Science Education and Research, Pune represents study/work carried out by Vaibhav Singh at the Indian Institute of Science Education and Research, Pune under the supervision of Anirban Hazra (Department of Chemistry, IISER Pune) and Spiridoula Matsika (Department of Chemistry, Temple University, Philadelphia, USA) during the academic year 2018-2019.



Vaibhav Singh



Spiridoula Matsika



Anirban Hazra

## Declaration

I hereby declare that the matter embodied in the report entitled *Interpreting Pump - Probe Experiments on Dimethyl Methyl Phosphonate (DMMP)* are the results of the work carried out by me at the Department of Chemistry, Indian Institute of Science Education and Research, Pune under the supervision of Anirban Hazra (IISER Pune) and Spiridoula Matsika (Temple University, Philadelphia, USA) and the same has not been submitted elsewhere for any other degree.



Vaibhav Singh



Spiridoula Matsika



Anirban Hazra

# Acknowledgements

First of all I would like to acknowledge my supervisors Anirban Hazra, IISER Pune and Spiridoula Matsika, Temple University, Philadelphia, USA for their immense support throughout the project. Without Dr. Hazra I would have not been able to explore this field of applications of quantum chemistry. It was his guidance in the early days of my joining the lab which is why I am able to reach at this point. On another hand the equal guidance and support by Prof. Matsika during my project work is nothing less than a blessing. I feel lucky to have such advisors. I am also thankful to Katharine Tibbetts, Virginia Commonwealth University, USA for performing experiments and verifying some of my results. I would also like to thank my TAC member Arun Venkatnathan, IISER Pune for support and advising me on the thesis work and report.

I would also like to thank my present and ex lab members Mahesh, Meghna, Avdhoot, Divya and Bappa for helping me with small, big and even silly doubts. Especially Mahesh and Meghna from Dr. Hazra group who have helped me with programming and learning basics about quantum calculations on molecules. They have always treated me like a kid and were always there when I needed them emotionally or academically. I would also like to thank my friends a lot who were there to support mentally if I got stuck with some problem.

Also, thanks to IISER Pune for providing such an amazing environment for research. I am also thankful to DST-INSPIRE and Infosys Foundation for providing me with INSPIRE and undergraduate fee-waiver scholarship respectively which were very helpful during my academic career.

Atlas though not in the order I would thank my parents and sister too who were always standing with me even at the tough situations. I thank them for understanding me and let me pursue with my interest of research.

# Contents

Certificate.....	3
Declaration.....	4
Acknowledgements.....	5
List of Figures .....	7
List of Tables .....	7
Abstract.....	8
1. Introduction .....	9
1.1 Pump-Probe Experiment.....	9
1.2 Scope of the Thesis .....	11
2. Methods.....	12
2.1 Hypothesis.....	12
2.2 Description of the Methods and Calculations.....	13
2.2.1 Hartree Fock (HF) Theory.....	14
2.2.2 Optimization .....	15
2.2.3 Linear Interpolation .....	16
2.3 Dyson Orbitals.....	19
3. Results and Discussions .....	21
3.1 Optimized geometries.....	21
3.2 Ionization potentials at $S_0$ and $D_0$ geometries .....	23
3.3 Geometries of Excitation Due to Probe Light .....	24
3.4 Experimental proofs.....	26
4. Future Perspectives.....	28
5. Conclusions .....	29
Appendix I .....	30
Appendix II .....	31
Appendix III .....	33
Appendix IV.....	35
References .....	37

## List of Figures

**Figure 1** Ultrafast Pump-Probe Experiment performed on the molecule DMMP.

**Figure 2** DMMP molecule

**Figure 3**  $\text{DMMP}^+$  is the major ion formed when ionized with 1200 and 1500 nm pump light.

**Figure 4** The number of oscillations when ionized with 1200 and 1500 nm pump light.

**Figure 5** Non-adiabatic (On left) and the Adiabatic Ionization (On right).

**Figure 6** Ion signals of  $\text{PO}_2\text{CH}_4^+$ ,  $\text{PO}_3(\text{CH}_3)_2^+$  and  $\text{PO}_2\text{C}_2\text{H}_7^+$  and  $\text{DMMP}^+$  against the pump-probe time delays.

**Figure 7** Schematic diagram for the hypothesis.

**Figure 8.1a** HF picture, lowest N orbitals occupied.

**Figure 8.1b** Singly excited case. Electron exciting from a<sup>th</sup> to p<sup>th</sup> orbital.

**Figure 9** Optimized structures of DMMP (left) and  $\text{DMMP}^+$  (right) in their respective ground states  $S_0$  and  $D_0$

**Figure 10** Pictorial representation of the IPs at both the neutral ( $S_0$ ) and cationic ( $D_0$ ) geometries

**Figure 11** DMMP Cation energies at linearly interpolated points

**Figure 12** Oscillator Strengths at linearly interpolated points between the  $S_0$  and  $D_0$  geometries

**Figure 13** Mass Spectra at 3 time delays (t)

**Figure 14** Oscillatory (dots) and the least squares fitted ion signals (solid lines).

**Figure 15** Ion signal of cations against the pump-probe time delays.

## List of Tables

**Table I** Internal coordinates of DMMP and  $\text{DMMP}^+$  optimized geometries.

**Table II.** Ionization potentials of DMMP at  $S_0$  and  $D_0$  geometries.

**Table III** IPs at different geometries.

## Abstract

Recently ultrafast pump-probe experiments have been performed on Dimethyl Methyl Phosphonate (DMMP) where the pump light was used to adiabatically ionize the molecule and the probe light was used to study the dynamics of the cations produced. There was an oscillatory behavior in the transient cation yield. Also an anti-phase relation was found between the yield of the parent molecular ion ( $\text{DMMP}^+$ ) and the other cation fragments. In this work a detailed study has been carried out to understand the experimental observations with the help of quantum chemical calculations. Ionization potentials of DMMP and the oscillator strength between the ground and excited electronic states of the cation were calculated. It seems that the probe light excites the  $\text{DMMP}^+$  to the 2<sup>nd</sup> and 3<sup>rd</sup> excited states ( $D_2$  and  $D_3$ ) where the molecule gets dissociated further. This happens for certain geometries of  $\text{DMMP}^+$  where the energies of  $D_2$  and  $D_3$  become resonant with the probe light. Hence the population of  $\text{DMMP}^+$  gets depleted giving rise to the dissociated ions. At the  $\text{DMMP}^+$  ground state geometry this resonance doesn't occur and hence there is transition causing no depletion of it.



# 1. Introduction

## 1.1 Pump-Probe Experiment

DMMP is a nerve agent simulant used for developing sensors for chemical warfare agents<sup>1</sup>. Exposure to these agents blocks the pathways through which the nervous system sends signals to the different parts of the body leading to paralysis and sometimes death<sup>2</sup>. A study of nerve agent simulants can help design probes for detecting these hazardous compounds.

Recently an ultrafast pump-probe experiment has been performed on DMMP in order to understand its radical cation dynamics<sup>3</sup>. The molecule was first ionized with high-intense strong field pump light varying from 800 to 1600 nm using multi-photon ionization where multiple laser photons were simultaneously exposed to the molecule in order to ionize it (Blue arrows in Figure 1). The dynamics of the resulting cation was probed with a weak probe pulse of 800 nm. (Red curved arrows in figure 1).

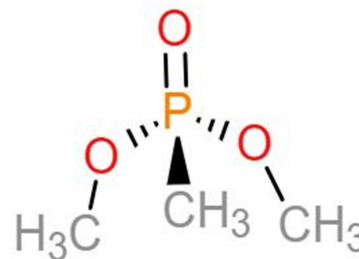
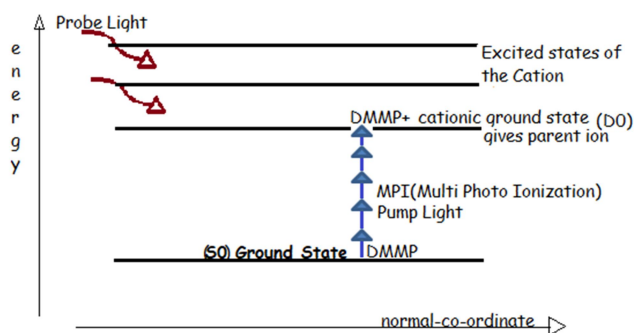


**Figure 1** Ultrafast Pump-Probe Experiment performed on the DMMP

**Figure 2** DMMP molecule<sup>3,4</sup>

One of the major challenges in these experiments is the preparation of chiseled initial coherent state to be formed after the ionization<sup>4</sup>. In this experiment the state is the cationic ground state which should be predominately populated by the parent ion which needs the lowest energy to get ionized from the neutral molecule. In the case of 800 nm pump light, there is extra energy available than what is just needed to form the parent ion. As a result, multiple major ions other than the parent ion are formed<sup>5</sup> (Figure 3).

This is non-adiabatic ionization<sup>5</sup>. This leads to the increased number of collisions and hence dissociations. This causes fast dephasing of the parent molecular ion DMMP<sup>+</sup> (Figure 4). But when the wavelength of the pump light was increased from 800 nm to in between near infrared region (1200 nm - 1500 nm) the major ion formed was the parent ion (Figure 3). The number of clearly visible oscillations has also been increased approximately from 6 to 12 implying better and improved coherence in the latter case (Figure 4). This is adiabatic ionization<sup>5</sup>. The strong laser field potential bends the coulombic potential of the molecule and hence allows the electron to tunnel out through the potential barrier (Figure 5) with just enough energy required to produce the parent ion.

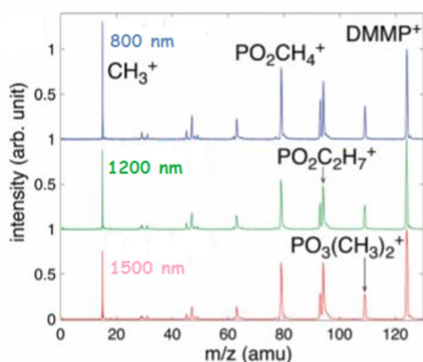


**Figure 3** DMMP<sup>+</sup> is the major ion formed when ionized with 1200 and 1500 nm pump light. (Tibbetts, 2018)<sup>3</sup>

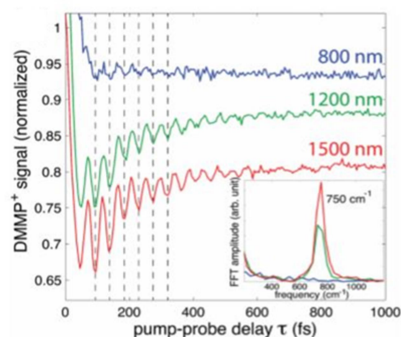


**Figure 4** The number of oscillations increases when ionized with 1200 and 1500 nm pump light. (Tibbetts, 2018)<sup>3</sup>

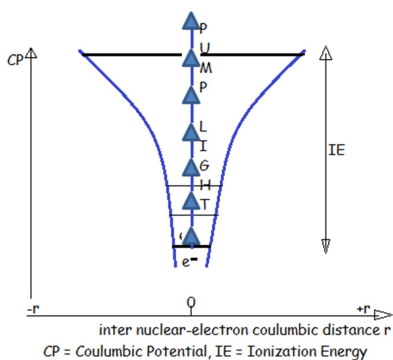


**Figure 5.1** Non-adiabatic Ionization.

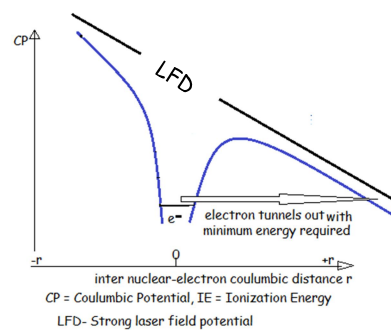


**Figure 5.2** Adiabatic Ionization.

The ion-signals of three major ions  $\text{PO}_2\text{CH}_4^+$ ,  $\text{PO}_3(\text{CH}_3)_2^+$  and  $\text{PO}_2\text{C}_2\text{H}_7^+$  have been plotted against the pump-probe time delays other than the DMMP+ and the result is shown in Figure 6<sup>3</sup>.

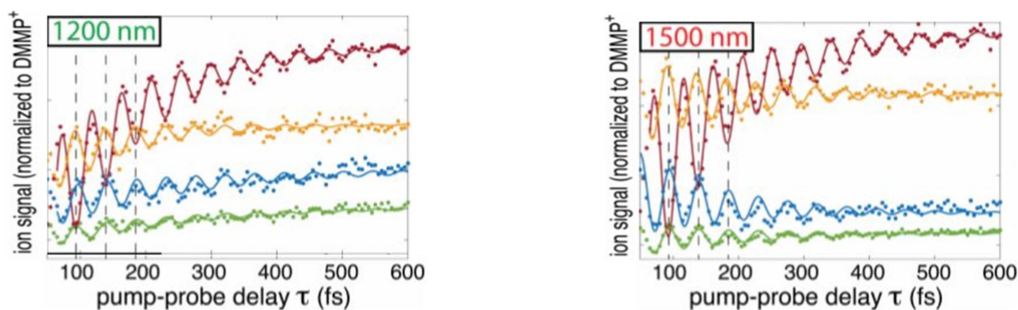


**Figure 6** Ion signals of  $\text{PO}_2\text{CH}_4^+$ ,  $\text{PO}_3(\text{CH}_3)_2^+$  and  $\text{PO}_2\text{C}_2\text{H}_7^+$  and  $\text{DMMP}^+$  against the pump-probe time delays (Tibbetts, 2018)<sup>3</sup>.

## 1.2 Scope of the Thesis

The oscillatory behavior can be clearly seen in the wave packet dynamics of the cations against the time delays (Figures 4 and 6). The question which now can be asked is, ‘why there is an oscillatory behavior in the wave packets’. Also, when the ion signals of  $\text{PO}_2\text{CH}_4^+$ ,  $\text{PO}_3(\text{CH}_3)_2^+$  and  $\text{PO}_2\text{C}_2\text{H}_7^+$  were plotted against the probe time delays, there is an anti-phase relation between the wave packets of these 3 and the  $\text{DMMP}^+$  ion signal (Figure 6). Why is there an anti-phase relation between the wave packets of parent ion and the secondary cations? The approach and hypothesis to answer the questions have all been addressed in the next section. The pathways through which the cations form or dissociate into other cations have not been covered in this work. The ‘Results and Discussions’ section will mainly have the results (both experimental and computational) supporting the hypothesis for the first question and then followed by the ‘Conclusion and Future Perspectives’ concluding the thesis work.

## 2. Methods

To understand the oscillatory behavior of the wave packet dynamics of the cations, a hypothesis is proposed in section 2.1. Also, different quantum chemical calculations were performed on the molecule to verify whether the hypothesis is correct or not. These calculations are based on multiple electronic structure theories which are also discussed in the later sections.

### 2.1 Hypothesis

As discussed earlier, the pump first ionizes the neutral Dimethyl methyl Phosphonate (DMMP) using either the adiabatic or non-adiabatic ionization. The non-adiabatic ionization wasn't able to provide the desired coherence in the wave packets of the cations. Hence it was ionized adiabatically. Hypothesis is that when the DMMP is ionized and cations are formed, the probe light then excites the  $\text{DMMP}^+$  from its ground state to the higher excited state where further dissociation occurs (Figure 7). Few questions can be asked now. First, to which state and at what geometry is the pump light ionizing the molecule? The answer is the experimentalists have pumped the molecule when it is in its lowest energy state, i.e. when it is at the minima of ground state energy. This is called the optimized geometry of a molecule. Note that after the ionization, the cation may not be in its optimized geometry and it can relax to its own equilibrium geometry. This newly formed cation would have its own ground state and excited states. Second, to which state and at what geometry is the probe light exciting the  $\text{DMMP}^+$  from its ground state? This is the question which is addressed in detail in this work. So the hypothesis is that initially DMMP is ionized at its ground state geometry (optimized DMMP geometry in its ground state  $S_0$ ). Then the  $\text{DMMP}^+$  relaxes to its minimum geometry and in course gets excited to the higher state when the probe light resonates with the energy gap between these two energy states at some geometry (Figure 7). The maximum depletion in the  $\text{DMMP}^+$  population occurs at these time delays. There must be a geometry where the excited states would have been out of reach of the probe light, hence causing no transitions. The  $\text{DMMP}^+$  population is the

maximum at these particular time delays. It is also hypothesized that when  $\text{DMMP}^+$  population depletes, it is formed into other cations. Hence there is an anti-phase relation which was talked about in figure 6 in the previous section. Another question which arises is the pathway by which the  $\text{DMMP}^+$  dissociates into secondary ions and then relaxes back after introducing probe light. This pathway may include conical intersections where Born-Oppenheimer approximation<sup>6</sup> (explained later) fails and the two potential surfaces (or energy states) meet. This question has not been addressed so much but will be touched in the 'Future Perspectives' section.

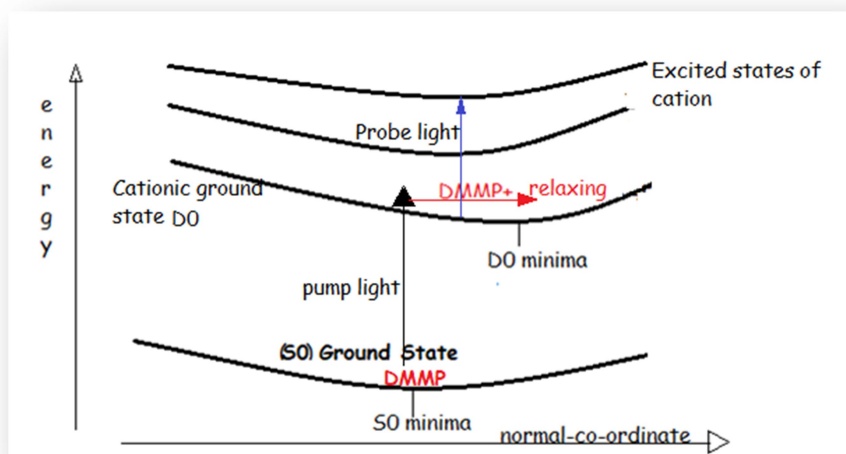


**Figure 7** Schematic diagram for the hypothesis. An S0 minimum is where DMMP is in its minimum energy, D0 minima is where  $\text{DMMP}^+$  is in its minimum energy.

## 2.2 Description of the Methods and Calculations

In order to understand the electronic states of the molecule or atom, one has to solve the time-independent Schrödinger equation. Finding its solutions is simple for Hydrogen like atoms but gets complicated for many electron or polyatomic systems. Hence approximations are made in order to solve it. One of them is the Born Oppenheimer (BO) approximation<sup>6</sup>. The Schrödinger equation for  $j$  and  $i$  number of nucleus and electrons respectively is as follows: Hamiltonian (H),

$$(H) = \left[ \frac{-\hbar^2}{8\pi^2} \sum_j \frac{\nabla_j^2}{m_j} + \frac{-\hbar^2}{8\pi^2} \sum_i \frac{\nabla_i^2}{m_e} + V(R_j, r_i) \right] \varphi = E\varphi, H\varphi = E\varphi.$$

$$\text{Where, } \hat{T} = \frac{-\hbar^2}{8\pi^2} \sum_j \frac{\nabla_j^2}{m_j} + \frac{-\hbar^2}{8\pi^2} \sum_i \frac{\nabla_i^2}{m_e}; (T = \hat{T}_n + \hat{T}_e)$$

is the part describing the Kinetic energy of the nucleus and electron. 'm<sub>j</sub>' and 'm<sub>e</sub>' are the masses of j<sup>th</sup> nucleus and electron respectively. Also, V(r) describes the potential energy of the molecule. R<sub>j</sub> and r<sub>i</sub> are the positions of j<sup>th</sup> nucleus and i<sup>th</sup> electron respectively. The kinetic energy operator depends upon the position of the nuclei (R<sub>j</sub>) as well as the position of the electron (r<sub>i</sub>). Now, V(r) can be classified into 3 terms. First the electrostatic interactions between electron – electron (V<sub>e-e</sub>), second the electrostatic interaction between nuclei – electron (V<sub>n-e</sub>) and finally the electrostatic interaction between nuclei-nuclei (V<sub>n-n</sub>). This allows to write Hamiltonian into total 5 terms:

$$H = \hat{T}_n + \hat{T}_e + V_{e-e} + V_{n-e} + V_{n-n}$$

Since the electron is 1800 times lighter than a proton, electrons are way faster than protons. The positions of the nuclei can be hence fixed and this leaves the Hamiltonian only with 3 terms  $\hat{T}_e + V_{e-e} + V_{n-e}$ , leaving  $\hat{T}_n$  and  $V_{n-n}$  as constants because they depend only on R<sub>j</sub>. This is called the Born-Oppenheimer approximation, a very important assumption in solving any of the quantum chemical problems, and it has been used in all of my electronic state calculations. Next, Hartree Fock (HF) theory a self-consistent field (SCF) method which solves the Hamiltonian problem is being discussed. It also forms the basis for the other quantum performing methods. The whole derivation and details will not be discussed but some will be referenced to the sources.

### 2.2.1 Hartree Fock (HF) Theory

HF theory forms the basis for almost all of the other methods which is used to understand the electronic structure of a molecule. This makes it important to be discussed. It solves the Hamiltonian,  $H\varphi(r) = E\varphi(r)$  to get the HF energies which are the eigenvalues of the equation<sup>6</sup>. First the spin orbitals which are to be occupied by electrons are guessed using Roothaan's-Hartree Fock equations<sup>7</sup>. These spin orbitals

are the functionals which are the function of other function (depending on other parameters). These functionals should form the complete basis set, i.e. if  $\{\Phi_1, \Phi_2, \Phi_3, \dots, \Phi_K\}$  are the spin orbitals to be occupied by N electrons then  $\sum_{i=1}^K |\Phi_i\rangle\langle\Phi_i| = 1$ . Now, a Slater Determinant is formed using these orbitals which describes the wave function of the ground state ( $\varphi$ ) of a molecule (Equation 1). In the equation,  $r_1, r_2, r_3, r_4, \dots, r_N$  are the parameters defining positions of electron 1, 2, 3, 4, ..., N respectively. The HF problem is to find the spin orbitals constituting to the best Slater determinant and hence the best wave function defining the ground state of the molecule. By best it means the wave function which gives the lowest ground state energy.

$$\text{Equation 1 } \varphi = \frac{1}{N!} \begin{bmatrix} \Phi_1(r_1) & \cdots & \Phi_K(r_1) \\ \vdots & \ddots & \vdots \\ \Phi_1(r_N) & \cdots & \Phi_K(r_N) \end{bmatrix}$$

These spin orbitals basically describe the molecular orbitals of the molecules and are solved using Roothaan's-Hartree Fock equations<sup>7</sup>. Also the Slater determinant formed by these orbitals is anti-symmetric which is desired to form exact wave function (Refer Figure 19 discussed later). Anti-symmetric property here means when the orbitals of two electrons are exchanged, the wave function of the Slater determinant changes its sign<sup>6</sup>. Hence these spin orbitals are used in other methods like CCSD (Coupled Cluster Singles and Doubles), CI (Configurational Interaction) etc. for the calculation of excited states and other properties.

### 2.2.2 Optimization

First of all the optimized geometry of DMMP was required at which the pump light is ionizing it. The optimization was performed at Density functional theory-Restricted B3LYP (RB3LYP)<sup>8</sup> level of theory using 6-311+G(d)<sup>9</sup> as a basis set with the help of Gaussian09 suite of programs<sup>17</sup>. DMMP has singlet multiplicity (neutral molecule) and a total of 66 electrons. Hence the ground state of DMMP is called S0, where S stands for singlet and 0 for the ground state and the excited states are called S1, S2, S3 etc. The DMMP<sup>+</sup> having doublet multiplicity (one unpaired electron) and a

total of 65 electrons was also optimized using the same level of theory and software except Unrestricted B3LYP was used (UB3LYP). The ground state of DMMP<sup>+</sup> is called D<sub>0</sub> (D for Doublet). The motivation behind using this method was to reproduce the optimized geometries of the isomers of DMMP and DMMP<sup>+</sup> which has already been published using the same level of theory and software<sup>10</sup>. The comparison of the reproduced and the original result has been tabulated in Appendix I. It also gives more accurate results than HF theory in terms of energy.

Density Functional Theory (DFT)-B3LYP is a hybrid DFT- HF method. DFT method just uses the electron density functionals and does not need wave function to solve the Hamiltonian. One of the demerits of HF theory is that it does not account the electron dynamic correlation which DFT can with the help of approximations which makes it slightly better than HF<sup>11</sup>. One of the approximations uses Becke's 3 parameters with LYP (B3LYP) to solve correlation term and exchange term with the help of Slater determinant (hence hybrid)<sup>8</sup>.

### 2.2.3 Linear Interpolation

After the DMMP and DMMP<sup>+</sup> geometries were optimized, the aim was to build the similar picture as that made in the hypothesis. Henceforth, the optimized geometry of DMMP and DMMP<sup>+</sup> in their ground state will be called as S<sub>0</sub> and D<sub>0</sub> geometry (or neutral and cationic geometry) respectively. To have an approximate picture, the ionization potentials (IPs) of DMMP at both of the S<sub>0</sub> and D<sub>0</sub> geometries were needed. These IPs would then be verified with the larger basis set giving more accurate results. All the IPs at both the geometries were first calculated at Equations Of Motion-Ionization Potential-Coupled Cluster Singles and Doubles (EOM-IP-CCSD)<sup>12</sup>/6-311+G\*<sup>9</sup> level of theory using Q-Chem<sup>18</sup> software. The verification was done with the same method and software except the larger basis set cc-pVTZ was used. Due to the higher computational cost this basis set was not used later. Once the IPs were calculated, the next step was to linearly interpolate the IPs in between these two geometries S<sub>0</sub> and D<sub>0</sub>. This was done by calculating IPs of 9 geometries of DMMP in between two geometries. To get the 9 geometries in between the following formula was used:-



Assume that the molecule has 'n' number of internal co-ordinates. The geometries corresponding to the neutral and cationic geometry are also available. Let the internal co-ordinates be  $(a_1, a_2), (b_1, b_2), (c_1, c_2), \dots, (n_1, n_2)$  where in  $(x_1, x_2)$ , 'x $\in$ [a,n]' corresponds to the internal mode (bonds, angles, dihedrals) and  $x_1$  and  $x_2$  are the values at neutral and cationic geometry respectively. Now if one wants 9 geometries in between, one can get the step size for each internal mode as  $s(i) = \frac{abs(x_2 - x_1)}{10}$ , and then  $x_1 + (1*s_1), x_1 + (2*s_2), \dots, x_1 + (9*s_2)$  give values of internal coordinates at all the 9 geometries.

This is BO approximation. The nuclei of DMMP were frozen (by making the internal co-ordinates constant) and then IPs were calculated at all the 9 geometries. Oscillator strengths<sup>13</sup> were also calculated for the transitions in between  $D_0$  and the higher excited states at all the geometries. The oscillator strength tells us about the probability of whether transition will occur in between the given states. EOM-IP-CCSD cannot calculate the oscillator strengths since the reference state used is the  $S_0$ . Hence a similar method EOM-EE-CCSD<sup>12</sup> was used, where EE stands for Excited Energies. It simply calculates the excited energies for the DMMP<sup>+</sup> and then calculates the oscillator strength by calculating the transitional dipole moment between reference state (here  $D_0$ ) and the higher excited state. The difference between EOM-IP-CCSD and EOM-EE-CCSD has been discussed later in the section.

Coming on to the method both EOM-IP and EOM-EE uses the HF spin orbitals for the calculations which had been discussed in section 2.2.1. Figure 8 gives the pictorial idea of these spin orbitals. The notations similar to section 2.2.1 will be used. Here, the lowest N orbitals in energy are occupied out of total K orbitals called occupied orbitals. The rest of them [N-K] orbitals are called the virtual orbitals which are not occupied initially. The HF picture is shown in Figure 8.1, where lowest N orbitals are occupied by N electrons. The Slater determinant expressing the HF ground wave function has the short hand notation,  $\varphi = |\Phi_1 \Phi_2 \dots \Phi_a \Phi_b \dots \Phi_N\rangle$ . Now assume that an electron from any of the occupied orbital gets excited to any of the virtual orbital, for example electron in a<sup>th</sup> orbital gets excited to p<sup>th</sup> orbital. These are called single excitations and the new Slater determinant formed is called singly excited Slater

determinant. It is expressed as  $\varphi = |\Phi_1 \Phi_2 \dots \Phi_p \Phi_b \dots \Phi_N\rangle$ . Taking all the combinations of the single excitations, the combinations of singly excited Slater determinants are formed. Similarly, two and then three electrons can be excited to the virtual orbitals in order to get doubly and triply excited Slater determinants which go on further till N-tuply excited determinants. Taking all the possible  ${}^K C_N$  combinations (N orbitals chosen out of total K), exact wave function ( $\varphi(\text{total})$ ) can be built for any of the state of the system (Equation 2).  $\varphi(\text{total})$  is written in terms of HF  $\varphi$ , singly excited determinants  $\varphi^{a,p}$  (excitation a to p), doubly excited determinants  $\varphi^{ab,pq}$  (excitation a,b to p,q) and goes on. Solving it gives the exact energies (eigen values) of the system.

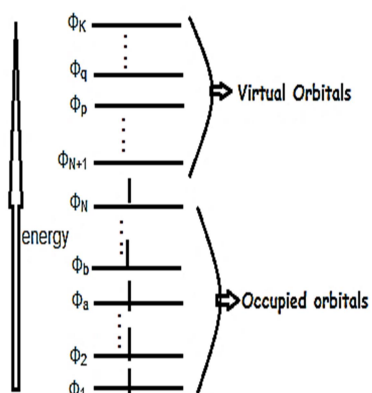


Figure 8.1a

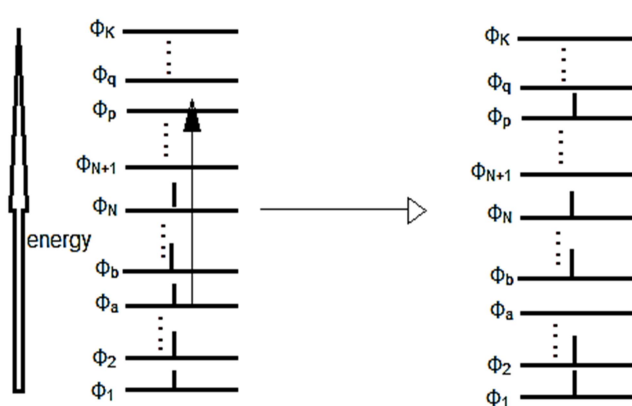


Figure 8.1b

**Figure 8.1a** HF picture, lowest N orbitals occupied. It describes the single Slater determinant  $\varphi$ .

**Figure 8.1b** Singly excited case. Electron exciting from a<sup>th</sup> to p<sup>th</sup> orbital.

Computationally, getting the exact energies is very hectic task and not possible. Hence what many methods like CCSD, CIS(D) (Configuration interaction singles and double) do is take only the singly and doubly excited determinants to form the wave function (up to 3<sup>rd</sup> term in Equation 2). Hence there is 'singles and doubles' in the name CCSD.

$$\text{Equation 2 } \varphi(\text{total}) = c_0 \varphi + \sum_a c_a |\varphi^{a,p}\rangle + \sum_{a,b} c_{ab} |\varphi^{ab,pq}\rangle + \sum_{a,b,c} c_{abc} |\varphi^{abc,pqr}\rangle + \dots$$

What CCSD uses is the fact that  $\varphi(\text{total})$  can be written as  $e^T\varphi$ , i.e. ' $\varphi(\text{total})= e^T\varphi$ '<sup>12</sup>, where  $T=T_1+T_2+T_3+\dots+T_i+\dots+T_N$ .  $T$  is the cluster operator where  $T_i$  generates all the i-tuply possible excited determinants. Since CCSD uses singles and doubles,  $T=T_1+T_2$  in this case. But when EOM is introduced another operator  $R$  plays important role.  $R$  is the general excitation operator. ' $R(0)\varphi$ ' means there is no change in the number of electrons in reference state (generally  $\varphi$ ) while calculating the excited energies of the system, this is EOM-EE-CCSD. ' $R(-1)\varphi$ ' means 1 electron has been taken out of the reference state now leaving the  $N-1$  electron basis set for the calculation. Calculations using  $R(-1)\varphi$  gives the corresponding ionization potentials of the system and is called EOM-IP-CCSD.  $R(+1)\varphi$  adds one electron to the system which gives the electron affinities (EAs) of a molecule. This is called EOM-EA-CCSD. In any of the EOM-CCSD methods the equation ' $\bar{H}R\varphi = ER\varphi$ ' is solved. Where,  $\bar{H}=e^{-T}He^T$  is the similarity transformation of Hamiltonian ( $H$ ) and  $E$  is the solution (excited energies or IPs) depending on the method being used. The EOM-IP and EOM-EE results<sup>14,15</sup> were also reproduced in order to get some confidence to apply these theories on DMMP. They are tabulated in Appendix II.

### 2.3 Dyson Orbitals

After the IPs are calculated, one can look at the orbitals from which the electrons have been ionized by calculating and visualizing the Dyson orbitals<sup>16</sup>. Dyson orbital is the overlap between the wave function of the  $N$ -electron system (from which the ionization occurs) and the wave function of the  $N-1$  electron system (formed after the ionization). This integrates out all the orbitals from which the ionization has not taken place leaving only the orbital or orbitals contributing to the ionized electron. If the multiple orbitals are contributing to the dyson orbital, (i.e. ionized electron density comes from one or two orbitals) it is represented as the linear combination of those orbitals pictorially representing 1 orbital. Mathematically, if  $\Phi(1,2,3,\dots,N)$  represents the wave function of the system initially before the ionization and  $\Phi(1,2,3,\dots,N-1)$  represents the wave function of the system after the ionization, then

$\varphi = \int [\Phi(1,2,3 \dots N) \Phi(1,2,3 \dots N - 1)] r(1)r(2)r(3) \dots r(N - 1)$  is the Dyson orbital calculated, where  $r(1), r(2), \dots, r(N)$  are the parameters defining the positions of  $N$  electrons. The Dyson orbitals contributing to the Ionization Potentials of DMMP at both the  $S_0$  and  $D_0$  geometries were calculated and have been tabulated in Appendix III. Dyson orbitals are either one of the HF orbital or the linear combination of them. This is reasonable because HF orbitals are used for the calculation of IPs.

### 3. Results and Discussions

This section starts with a discussion on the optimized geometries of DMMP and DMMP<sup>+</sup>. Then the results from the calculation of ionization potentials (IPs) of DMMP are discussed in section 3.2. In fact these IPs were the motivation to perform linear interpolation which had been discussed in 2.2.3. The results of this linear interpolation have been discussed next. The calculated oscillator strengths which seem to support the results of linear interpolation are also discussed. Finally, the experimental data (experiments done by Prof. Katharine Tibbetts) supporting the thesis work has been provided thus concluding this section.

#### 3.1 Optimized geometries

The internal co-ordinates (bonds and angles) of DMMP and DMMP<sup>+</sup> optimized geometries in their respective ground states are tabulated below in Table I. These geometries form the basis for all of the calculations ahead like linear interpolation, calculation of oscillator strengths etc. as explained in the Methods section. One can look at the optimized structures in figure 9, DMMP is totally an asymmetric molecule whereas DMMP<sup>+</sup> is more a symmetric one. Also to confirm that the structures belong to the true minima of their respective ground states ( $S_0$  and  $D_0$ ), IR frequencies were also calculated at B3LYP<sup>8</sup>/6-311+G<sup>\*9</sup> level of theory using Gaussian 09<sup>17</sup>. The frequencies are tabulated in appendix IV, and it could be observed that all of the normal modes are positive.



**Figure 9** Optimized structures of DMMP (left) and DMMP<sup>+</sup>(right) in their respective ground states  $S_0$  and  $D_0$ .

S.No.	Internal Coordinate	DMMP	DMMP <sup>+</sup>
1	R(1,2)	1.0882	1.0853
2	R(1,3)	1.4384	1.4703
3	R(1,4)	1.0913	1.0881
4	R(1,5)	1.0919	1.0883
5	R(3,6)	1.6111	1.5649
6	R(6,7)	1.4843	1.5815
7	R(6,8)	1.6269	1.5697
8	R(6,10)	1.8040	1.7751
9	R(8,9)	1.4376	1.4690
10	R(9,14)	1.0889	1.0884
11	R(9,15)	1.0933	1.0857
12	R(9,16)	1.0901	1.0879
13	R(10,11)	1.0907	1.0915
14	R(10,12)	1.0913	1.0913
15	R(10,13)	1.0901	1.0913
16	A(2,1,3)	106.2028	105.3521
17	A(2,1,4)	109.9061	110.8921
18	A(2,1,5)	109.7095	110.7827
19	A(3,1,4)	110.5913	110.4070
20	A(3,1,5)	110.2398	107.3830
21	A(1,3,6)	120.7336	131.4000
22	A(3,6,7)	116.8844	106.5593
23	A(3,6,8)	101.5322	116.6463
24	A(3,6,10)	100.6842	106.8093
25	A(7,6,8)	113.2904	104.0426
26	A(7,6,10)	116.4443	116.343
27	A(8,6,10)	106.1303	106.8686
28	A(6,8,9)	121.3216	131.6895
29	A(8,9,14)	106.4356	106.4461
30	A(8,9,15)	110.2900	105.8416
31	A(8,9,16)	110.7972	110.8015
32	A(4,1,5)	110.1180	111.8365
33	A(14,9,15)	109.3310	110.7999
34	A(14,9,16)	110.2883	111.6917
35	A(15,9,16)	109.6462	111.0084
36	A(6,10,11)	109.3239	109.0592
37	A(6,10,12)	109.0417	109.0714
38	A(6,10,13)	110.7539	109.8671
39	A(11,10,12)	108.6598	109.6462
40	A(11,10,13)	109.5157	109.4989
41	A(12,10,13)	109.5114	109.6818

**Table I** Internal coordinates of DMMP and DMMP<sup>+</sup> optimized geometries. R(a,b) corresponds to the bond length between a<sup>th</sup> and b<sup>th</sup> atom in Angstroms (Å). A(a,b,c) corresponds to the angle in between a<sup>th</sup>, b<sup>th</sup> and c<sup>th</sup> atom in degrees. For numbering of atoms refer to figure 8 of DMMP molecule.

### 3.2 Ionization potentials at $S_0$ and $D_0$ geometries

The ionization potentials of DMMP at both the neutral and cationic geometry are tabulated in Table II which can also be visualized in figure 10. These ionized states of DMMP are called  $D_0, D_1, D_2, \dots, D_n$ , where D stands for the doublet. At  $S_0$  geometry it can be clearly seen that the probe light (of 1.55 eV used in the experiment<sup>3</sup>) could only excite the  $DMMP^+$  from  $D_0$  to  $D_1, D_2$  and  $D_3$  because they are within 1.55 eV. While at  $D_0$  geometry, only  $D_1$  is in reach of the probe light. Also, note the nearly degenerate states  $D_0$  and  $D_1$  at neutral geometry which could mean cations are also formed at  $D_1$  state by the pump light. The  $D_0$  and  $D_1$  energies being less at  $D_0$  geometry than  $S_0$  geometry may suggest that the cations formed in these two states relax along  $S_0$  to  $D_0$  potential surface. While the  $DMMP^+$  relaxes, the probe light excites the molecule to the higher state at some geometry or one says probe light becomes resonant with the energy gap at that geometry. To know the geometry at which this resonance occur, the IPs at neutral and cationic geometry need to be connected. This is done by linearly interpolation of the IPs by the method discussed in the section 2.2.3 and has been discussed next.

States	Energies at neutral DMMP geometry(eV)	Energies at cationic geometry(eV)
1/A	10.313	9.431
2/A	10.406	9.809
3/A	10.911	11.503
4/A	11.491	12.104
5/A	12.029	13.230
6/A	12.562	13.459
7/A	13.715	14.430
8/A	14.253	14.967
9/A	14.732	15.596
10/A	15.317	16.102
11/A	15.388	16.679
12/A	15.776	16.775

**Table II.** Ionization potentials of DMMP at its optimized ground state geometry ( $S_0$ ) and at cationic geometry ( $D_0$ ).

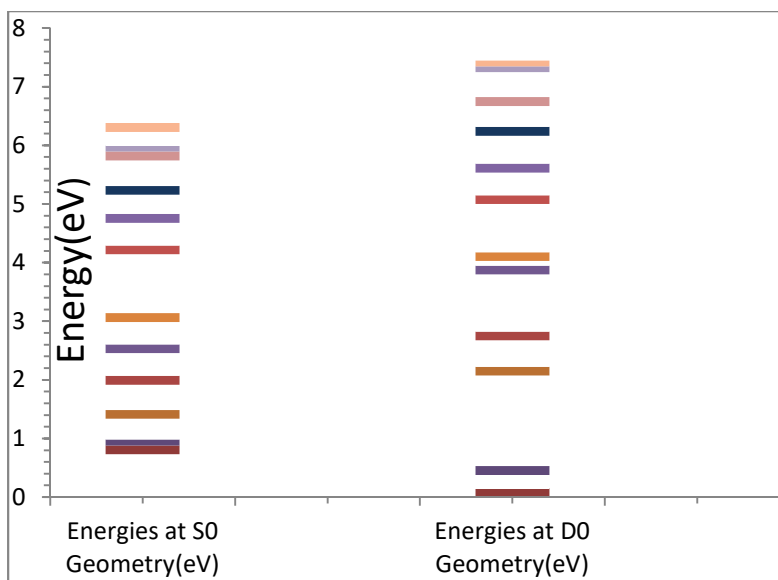


**Figure 10** Pictorial representation of the IPs at both the neutral ( $S_0$ ) and cationic ( $D_0$ ) geometries

### 3.3 Geometries of Excitation Due to Probe Light

The linearly interpolated IPs are shown in figure 11 for 10 geometries in between the neutral and cationic geometry. Note that only 4 cationic excited states are taken into account because the rest of them are not within reach of the probe light. But this does not confirm that the transition will occur at the geometry where the probe light resonates with the energy (E) gap  $[E(D)_n - E(D)_0]$ . For confirmation, oscillator strengths were calculated and plotted along all the 12 geometries (including neutral and cationic geometry) in figure 12. As said in the section 2.2.3 EOM-IP-CCSD couldn't calculate the oscillator strengths and hence EOM-EE-CCSD was used to calculate it. Here all the calculations were performed taking  $D_0$  as the reference state, i.e. oscillator strengths were calculated for transitions taking from  $D_0$  to  $D_n$  state only. Since EOM-EE-CCSD calculates the excited energies (EEs) and the oscillator strengths from cationic ground state to its excited states, the EEs should be fairly near to IPs. They are linearly interpolated for all the 12 geometries and is plotted in the same figure 11 using dashed lines. Also note that each EE and IP are within the 0.5 eV range of difference. The IPs are also tabulated in Table III. It could be clearly seen from the table that there are 2 instances where energy gap of 1.55 eV is achieved: first from  $D_0$  to  $D_3$  in between



geometries 1 and 3 (at point 2), second from  $D_0$  to  $D_2$  in between geometries 5 and 6. Also the oscillator strength gets maximum at these points (Figure 12) suggesting that the probe light might be getting resonant at these 2 instances and hence exciting the  $DMMP^+$ . This is why  $DMMP^+$  is depleted at these geometries forming into other cations at  $D_2$  and  $D_3$ . While at the relaxed ( $D_0$ ) geometry, none of the states are within the reach of the probe light hence causing no depletion in it.

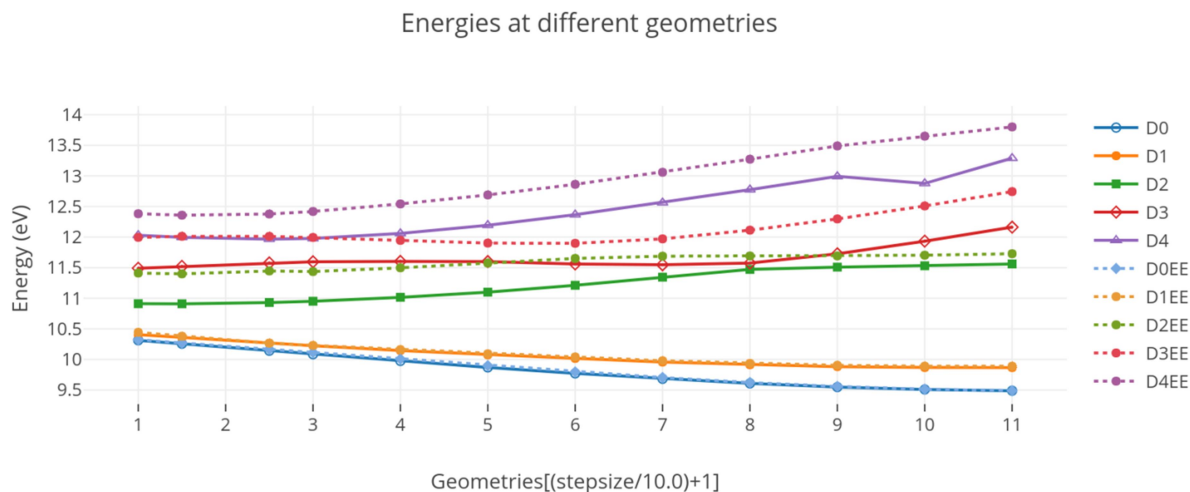


**Figure 11** DMMP Cation energies at linearly interpolated points, between the ground state geometry and cationic minimum energy geometry calculated at EOM-IP-CCSD (6-311+G(d), solid line) and EOM-EE-CCSD (6-311+G(d), dashed line) level of theory.

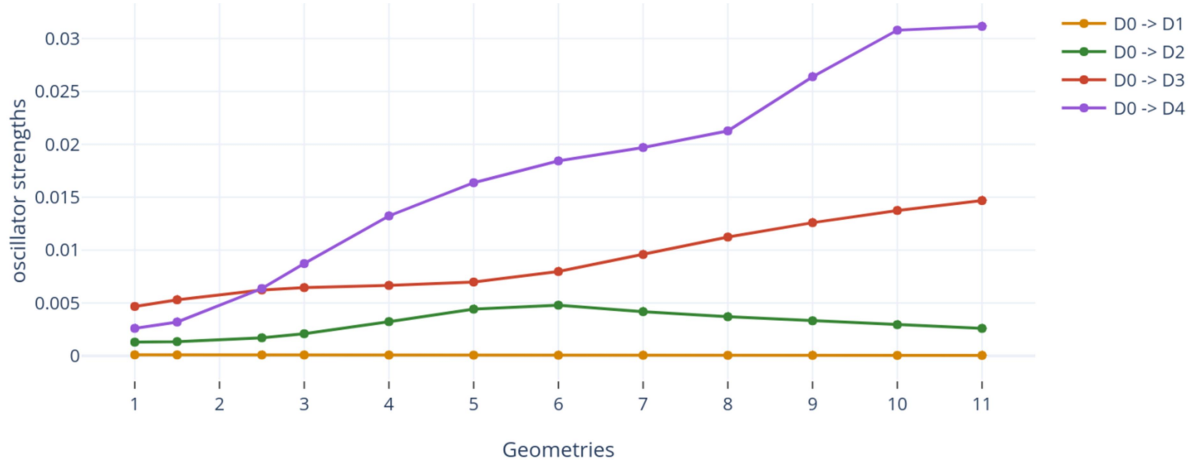


**Figure 12** Oscillator Strengths at linearly interpolated points between the ground state geometry and cationic minimum energy geometry. The points at 1.5 and 2.5 are the geometries with the step size of 5 (Refer sec. 2.2.3.)

IPs at $\rightarrow$ Geometries	$S_0$	1.5	2.5	3	4	5	6	7	8	9	10	$D_0$
<b>States</b> $\downarrow$												
$D_0$	0.824	0.767	0.653	0.596	0.487	0.381	0.283	0.194	0.119	0.059	0.020	0
$D_1$	0.917	0.867	0.776	0.734	0.657	0.586	0.528	0.468	0.425	0.394	0.379	0.378
$D_2$	1.422	1.421	2.442	1.462	1.527	1.611	1.723	1.856	1.982	2.020	2.042	2.072
$D_3$	2.002	2.032	2.089	2.107	2.114	2.111	2.072	2.058	2.086	2.238	2.444	2.673
$D_4$	2.541	2.508	2.478	2.488	2.570	2.705	2.877	2.073	3.286	3.502	3.388	3.800

**Table III** IPs at different geometries. The geometries 1.5 and 2.5 are produced by taking the step size of 5. Please refer section 2.2.3 for more details. All the energies are with respect to cationic geometry.

### 3.4 Experimental proofs

In this section, few experimental results will be discussed which are supporting some of the results from this thesis work. These experiments were performed by Prof. Katharine Tibbetts group, at Virginia Commonwealth University. Mass spectra at three pump-probe time delays  $t=-500$ fs,  $t=100$  fs and  $t=5000$  fs were carried out and are shown in figure 13. Here  $t=-500$ fs denotes the initial time where there is no probe and the signal has been only due to pump light. ' $t=100$  fs' is the time when the DMMP<sup>+</sup> has been in between  $S_0$  and  $D_0$  geometry and ' $t=5000$ fs' denotes the time when max population of the DMMP<sup>+</sup> would have been relaxed to  $D_0$  geometry.

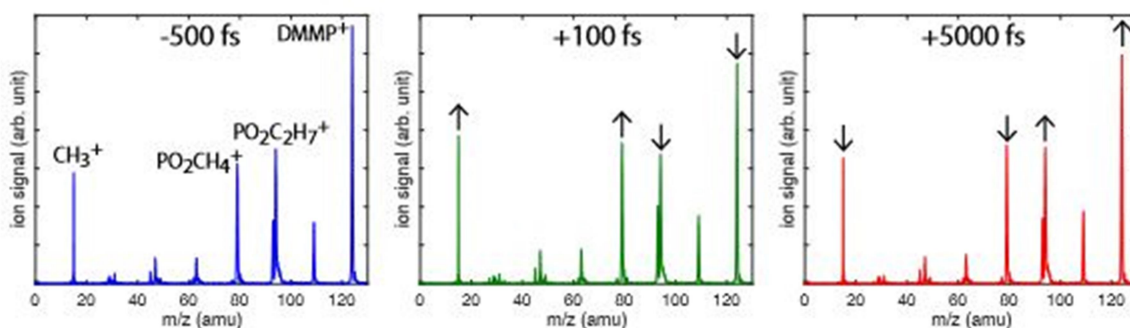


**Figure 13** Mass Spectra at 3 time delays (t)

The black arrows tell the increment (up) or decrement (down) in the particular ion. At 100 fs there is depletion in the DMMP<sup>+</sup> whereas at relaxed state ( $t=5000$ fs), there is

increment suggesting there is no exciting of  $\text{DMMP}^+$  in its relaxed state. This is something which has been discussed in the previous section.

The ion signals of parent and secondary radical cations ( $\text{DMMP}^+$ ,  $\text{PO}_2\text{C}_2\text{H}_4^+$  and  $\text{PO}_2\text{C}_2\text{H}_7^+$ ) were least square fitted against the function  $[a \cdot e^{-t/T} \sin(2\pi \cdot t/\tau + \gamma) + b]$ , where  $\tau$ =oscillatory period,  $a$ =Amplitude,  $T$ =Time period of the oscillation,  $\gamma$ =phase and  $b$  is value when  $\tau$  tends to infinity. This was then plotted by them as shown in figure 14. It can be observed from figure 14 that there is no exact anti phase relation between the wave packets of  $\text{DMMP}^+$  and the other ions. In fact they are close to  $\pi$ . The little difference (and not exact) in their anti-phase relation is due to the fact that  $\text{DMMP}^+$  is getting converted to these cations at different geometries which also have been discussed previously as a result of this thesis work.

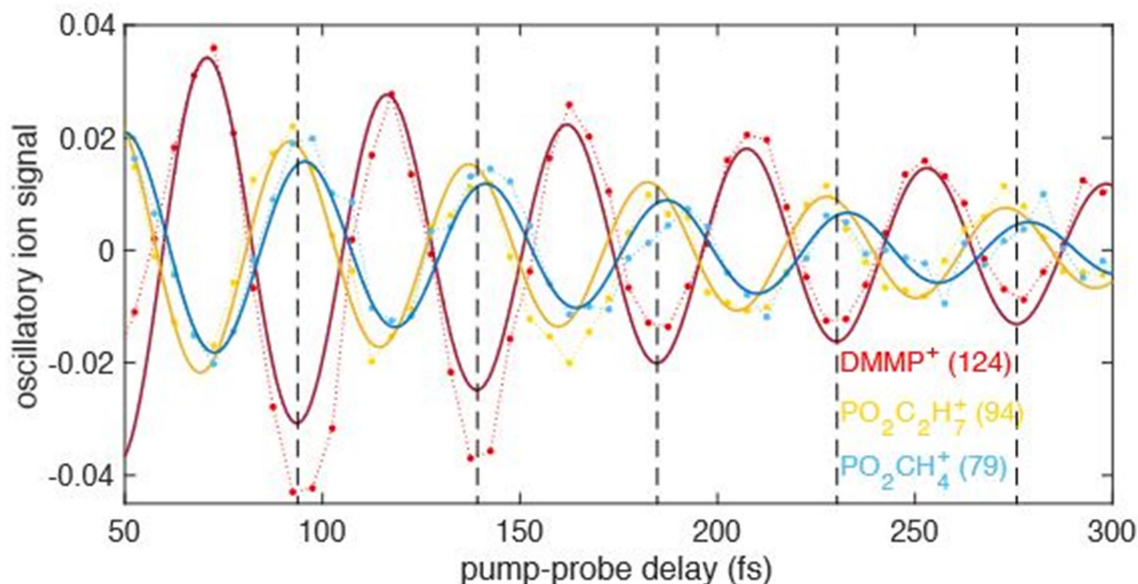


**Figure 14** Oscillatory (dots) and the least squares fitted ion signals (solid lines). (.)

These experimental results prove some of the results in this work which gives the confidence to have more calculations on DMMP and  $\text{DMMP}^+$  in future. One of them is finding the dynamics which has been discussed in the next section.

## 4. Future Perspectives

One of the important results to be observed in figure 10 is that the  $D_0$  and  $D_1$  energies are very close. As said already, it could be possible that pump light is also ionizing DMMP into  $D_1$  state. This gives rise to another possibility that probe light might excite the cation from this state. To confirm this, we need to calculate the oscillator strengths from  $D_1$  to the higher excited states. This is not possible with single reference methods like CCSD, CI etc. where generally, their ground state is taken as the reference state. Hence calculations have to be performed using multi reference methods<sup>6</sup> like CASSCF (Complete Active space Self-Consistent field), Multi Reference Configuration Interaction (MRCI) etc. Look at one of the results by Katherine group shown in figure 15.

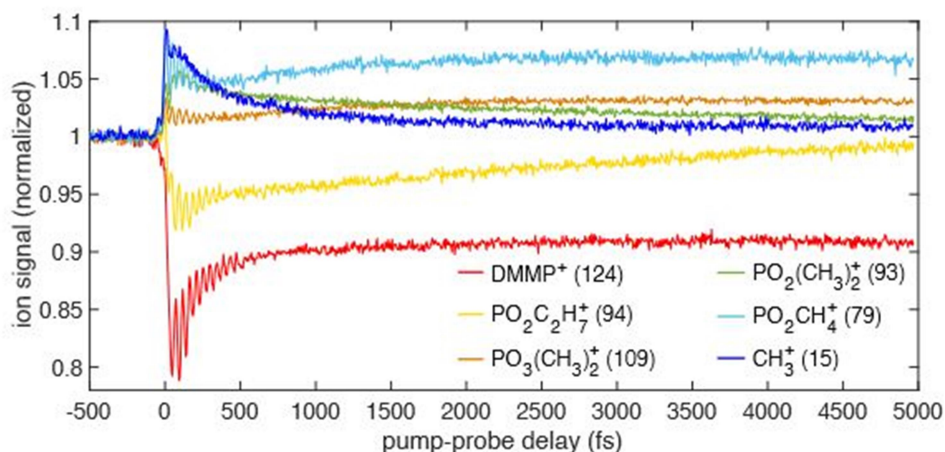


**Figure 15** Ion signal of cations against the pump-probe time delays.

It suggests that at longer time delays, where other cations signal flatten out, the signal for  $\text{PO}_2\text{C}_2\text{H}_7^+$  keeps increasing and that of  $\text{PO}_2(\text{CH}_3)_2^+$  keeps decreasing. It might be happening that  $\text{PO}_2(\text{CH}_3)_2^+$  gets converted into  $\text{PO}_2\text{C}_2\text{H}_7^+$  through some unknown pathway involving conical intersection (and hence the population decreases and increases respectively for  $\text{PO}_2(\text{CH}_3)_2^+$  and  $\text{PO}_2\text{C}_2\text{H}_7^+$ ). The work is in process and hopefully we will get more positive results soon.

## 5. Conclusions

The majority of the work in this thesis has been done to understand and interpret the ultrafast pump probe spectroscopy on Dimethyl Methyl Phosphonate. When ionized into its radical cation  $\text{DMMP}^+$ , the hypothesis was made that the probe light might be exciting it to its excited state where further dissociation occurs. There was also an anti-phase relation between the wave packets of  $\text{DMMP}^+$  and other cations which had no explanation before this work was carried out.

To understand the oscillatory behavior and anti-phase relation, the Ionization Potentials of DMMP were calculated giving some idea of the states to which the probe light might have been exciting the  $\text{DMMP}^+$  to from its ground state. From the calculations it was found that there were no states in reach of probe light at cationic geometry except  $D_1$ , whereas there were 3 excited states within the reach of probe light at neutral geometry. Hence linear interpolation of IPs was done along the geometries in between neutral and cationic geometry. The oscillator strengths for transitions from  $D_0$  to higher excited states were also calculated for all the geometries. The oscillator strengths for  $D_0$  to  $D_1$  transitions were very low implying no transition in between these states. But the oscillator strengths were able to verify the result that probe light gets resonated in between geometry 5 and 6 for  $D_0$  to  $D_2$  transition and in between geometry 1.5 and 2.5 for  $D_0$  to  $D_3$  transition. These are the geometries or the pump-probe time delays where  $\text{DMMP}^+$  population depletes (and the secondary ions form), whereas when it is in its relaxed state, it has the maximum population (and other ions population are at its minima of the oscillation). Hence they show the anti-phase oscillatory behavior. Also, the  $D_0$  and  $D_1$  energies were found to be so close at neutral geometry that it could even be possible for the pump light to ionize DMMP to  $D_1$ , implying probe light might also excite the cations from this state. The calculation of oscillator strengths from  $D_1$  to the higher states is currently under progress. The pathway and dynamics by which the cations are getting formed and destroyed into each other have also not been carried out in this work. This will also be addressed in future by calculating the conical intersections and other required calculations using multi reference methods.

## Appendix I

Table 1: Energies of the optimized geometries of DMMP isomers calculated in this work versus that in the paper (Gutsev and Tibbetts,) <sup>10</sup>.

S. no.	Isomer no.	Energy(eV) (Reproduced)	Energy from paper (eV)
1	I	0.0	0.0
2	II	0.11	0.11
3	III	0.22	0.22
4	IV	0.46	0.46
5	V(DMMP)	0.47	0.47
6	VI	0.47	0.47
7	VIII	0.53	0.53
8	IX	0.57	0.57
9	X	0.59	0.59
10	XI	0.63	0.63

Table 2: Energies of the optimized geometries of DMMP<sup>+</sup> isomers calculated in this work versus that in the paper (Gutsev and Tibbetts,) <sup>10</sup>.

S. no.	Isomer no.	Energy(eV) (Reproduced)	Energy from paper (eV)
1	I	0.0	0.0
2	II	0.04	0.04
3	III	0.07	0.07
4	IV	0.25	0.25
5	V	0.36	0.36
6	VI	0.43	0.43
7	VII	0.44	0.44
8	VIII	0.44	0.44
9	XIV	0.99	0.99
10	XV(DMMP <sup>+</sup> )	0.99	0.99

All the calculations were performed at B3LYP/6-311+G\* level of theory using Gaussian suites of program.

## Appendix II

The EOM-IP-CCSD and EOM-EE-CCSD results were reproduced from the papers (Levchenko and Krylov, 2006)<sup>14</sup> (Table I) and (Musia and Barlett, 2004)<sup>15</sup> (Table II) respectively.

1) EOM-IP-CCSD recalculations were done on formaldehyde and ethylene and are tabulated below.

i) Ethylene

S. no.	State	Energy(eV) (Reproduced)	Energy from paper (eV)
1	B <sub>3u</sub>	10.66	10.65
2	B <sub>3g</sub>	13.25	13.12
3	A <sub>g</sub>	14.65	14.89
4	B <sub>2u</sub>	16.51	16.30
5	B <sub>1u</sub>	19.47	19.62

ii) Formaldehyde

S. no.	State	Energy(eV) (Reproduced)	Energy from paper (eV)
1	1B <sub>2</sub>	10.71	10.70
2	1B <sub>1</sub>	14.30	14.29
3	2B <sub>1</sub>	15.75	15.74
4	2B <sub>2</sub>	17.91	17.90
5	3B <sub>1</sub>	21.56	21.89

All the calculations were performed at EOM-IP-CCSD/cc-pVTZ level of theory using Q-Chem. The slight differences in both the columns are due to the fact that the authors of the paper have used ACES suites of program and not Q-Chem.

## Appendix II

2) EOM-EE-CCSD recalculations were done on NO dimer<sup>15</sup> and are tabulated below.

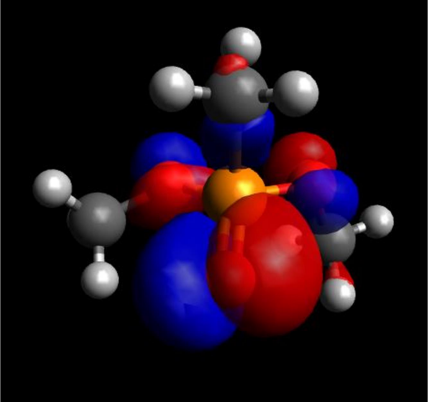
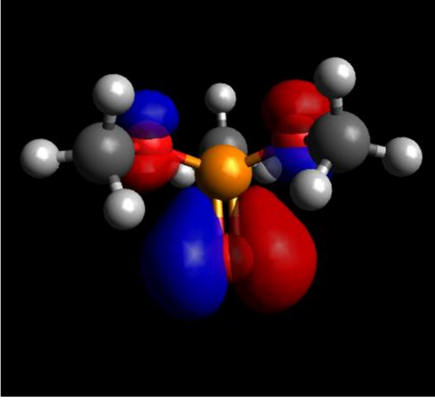
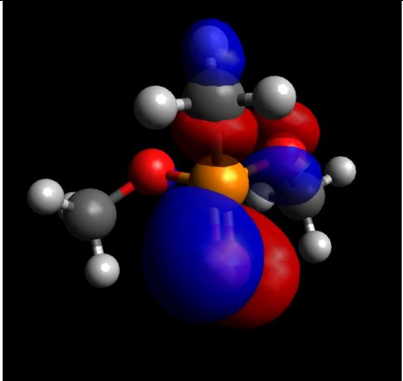
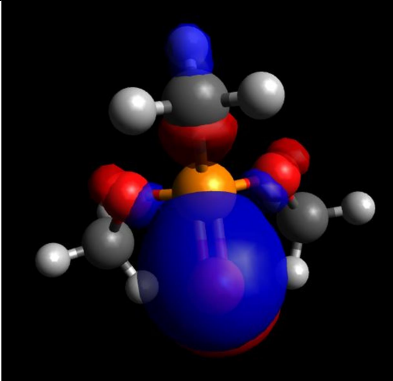
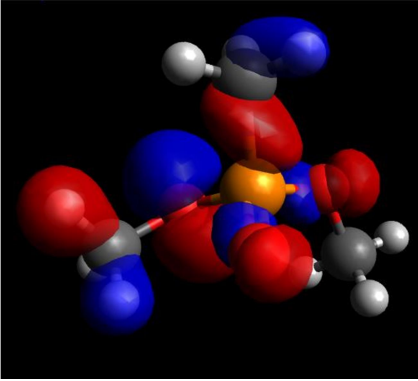
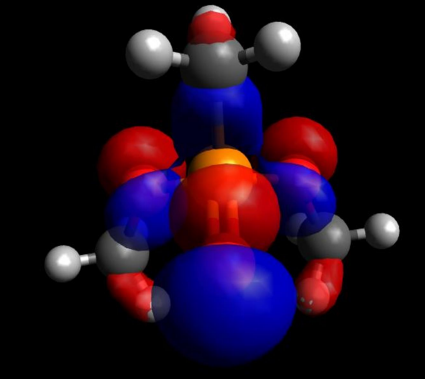
S. no.	State	Energy(eV) (Reproduced)	Energy from paper (eV)
1	1 <sup>1</sup> A <sub>1</sub>	5.56	5.56
2	2 <sup>1</sup> A <sub>1</sub>	6.27	6.27
3	3 <sup>1</sup> A <sub>1</sub>	7.12	7.12
4	1 <sup>1</sup> B <sub>1</sub>	6.18	6.18
5	2 <sup>1</sup> B <sub>1</sub>	7.53	7.53
6	3 <sup>1</sup> B <sub>1</sub>	8.01	8.01
7	1 <sup>1</sup> B <sub>2</sub>	6.10	6.10
8	2 <sup>1</sup> B <sub>2</sub>	6.42	6.42
9	3 <sup>1</sup> B <sub>2</sub>	7.38	7.38
10	1 <sup>1</sup> A <sub>2</sub>	7.20	7.20
11	2 <sup>1</sup> A <sub>2</sub>	7.44	7.44
12	3 <sup>1</sup> A <sub>2</sub>	8.24	8.24

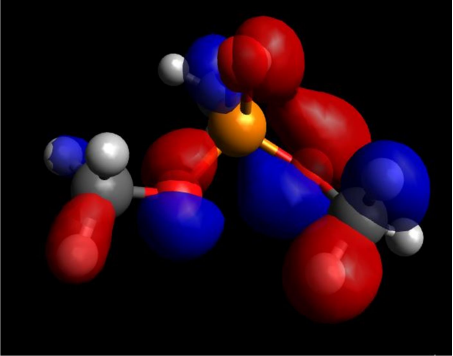
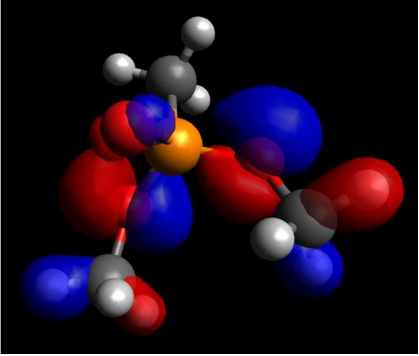
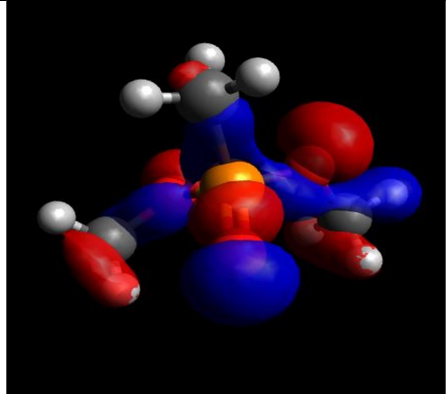
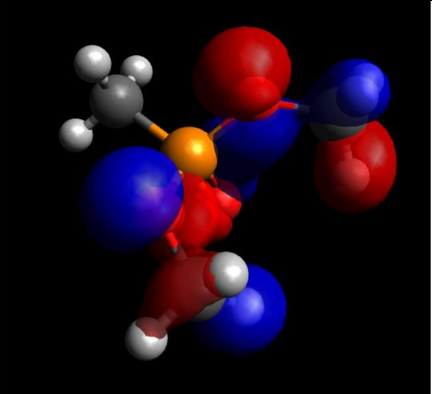
All the calculations were performed at EOM-IP-CCSD/6-311(2+)G(2df) level of theory using Q-Chem.



## Appendix III

The Dyson orbital contributing to the first 5 IP states were plotted for both of the geometries(S0 and D0) and are listed below :

States	Orbital contributing at S0 geometry	Orbital contributing at D0 geometry
1/A		
2/A		
3/A		

4/A		
5/A		

## Appendix IV

The IR frequencies for DMMP and DMMP<sup>+</sup> are tabulated below. Note that all of them are positive. All the calculations were performed at B3LYP<sup>8</sup>/6-311+G\* level of theory.

S.No.	IR Frequencies of DMMP (cm <sup>-1</sup> )	IR Frequencies of DMMP <sup>+</sup> (cm <sup>-1</sup> )
1	63.5060	20.6252
2	82.7246	61.2414
3	99.6889	85.1543
4	119.7474	106.1990
5	173.1968	136.3895
6	176.3160	155.0566
7	221.1858	166.6570
8	255.1275	208.0217
9	292.4866	253.2702
10	387.2925	271.9138
11	462.2476	346.1474
12	481.6043	471.8174
13	685.4424	659.4508
14	767.2050	756.1664
15	801.2874	771.7925
16	928.7518	864.0226
17	943.9277	933.8981
18	1056.7292	953.7652
19	1082.0808	1043.7528
20	1182.6986	1066.7284
21	1186.4227	1164.7048
22	1204.4534	1168.1510
23	1206.4944	1192.7659
24	1250.0132	1193.6992
25	1362.9135	1376.0280
26	1474.4438	1454.2342
27	1479.2109	1454.7505
28	1484.5402	1475.8303
29	1488.3808	1477.9303
30	1510.8355	1481.4026
31	1512.9846	1490.6092
32	1519.1945	1502.6054
33	1521.3009	1508.4522

## Appendix IV

The IR frequencies for DMMP and DMMP<sup>+</sup> (continued)

34	3039.0638	3059.9423
35	3045.6715	3078.7712
36	3057.8516	3080.3442
37	3116.0426	3149.4566
38	3120.2614	3151.5788
39	3137.6440	3177.8812
40	3147.2472	3178.2200
41	3147.5322	3199.7905
42	3149.9423	3203.7316

## References

1. Kuca K, Pohanka M. Chemical warfare agents. *BJAED*. 2010;100(6):543-558. doi:10.1007/978-3-7643-8338-1\_16
2. Gordon JJ, Inns RH, Johnson MK, et al. The delayed neuropathic effects of nerve agents and some other organophosphorus compounds. *Arch Toxicol*. 1983;52(2):71-82. doi:10.1007/BF00354767
3. Ampadu Boateng D, Gutsev GL, Jena P, Tibbetts KM. Ultrafast coherent vibrational dynamics in dimethyl methylphosphonate radical cation. *Phys Chem Chem Phys*. 2018;20(7):4636-4640. doi:10.1039/c7cp07261a
4. Bohinski T, Moore Tibbetts K, Tarazkar M, Romanov DA, Matsika S, Levis RJ. Strong field adiabatic ionization prepares a launch state for coherent control. *J Phys Chem Lett*. 2014;5(24):4305-4309. doi:10.1021/jz502313f
5. Stolow A, Rayner DM, Blanchet V, Villeneuve DM, Ivanov MY, Lezius M. Nonadiabatic Multielectron Dynamics in Strong Field Molecular Ionization. *Phys Rev Lett*. 2002;86(1):51-54. doi:10.1103/physrevlett.86.51
6. Cramer CJ. *Essentials of Computational Chemistry: Theories and Models.*; 2004. doi:10.1021/ci010445m
7. Roothaan C.C.J. Department of Physics, University of Chicago, Chicago, Illinois INTRODUCTION. 1951;(2). doi:10.1103/RevModPhys.23.69
8. Becke AD. Density-functional thermochemistry. III. The role of exact exchange. *J Chem Phys*. 1993;98(7):5648-5652. doi:10.1063/1.464913
9. Krishnan R, Binkley JS, Seeger R, Pople JA. Self-consistent molecular orbital methods. XX. A basis set for correlated wave functions. *J Chem Phys*. 1980;72(1):650-654. doi:10.1063/1.438955
10. Gutsev GL, Ampadu Boateng D, Jena P, Tibbetts KM. A Theoretical and Mass Spectrometry Study of Dimethyl Methylphosphonate: New Isomers and Cation Decay Channels in an Intense Femtosecond Laser Field. *J Phys Chem A*. 2017;121(44):8414-8424. doi:10.1021/acs.jpca.7b08889
11. Lee C, Hill C, Carolina N. Development of the Colle-Salvetti correlation-energy formula into a functional of the electron density. *Chem Phys Lett*.

- 1989;162(3):165-169. doi:10.1016/0009-2614(89)85118-8
12. Krylov AI. Equation-of-Motion Coupled-Cluster Methods for Open-Shell and Electronically Excited Species: The Hitchhiker's Guide to Fock Space. *Annu Rev Phys Chem.* 2008;59(1):433-462.  
doi:10.1146/annurev.physchem.59.032607.093602
  13. Harris RA. Oscillator strengths and rotational strengths in hartree-fock theory. *J Chem Phys.* 1969;50(9):3947-3951. doi:10.1063/1.1671653
  14. Levchenko S V., Reisler H, Krylov AI, et al. Photodissociation dynamics of the NO dimer. I. Theoretical overview of the ultraviolet singlet excited states. *J Chem Phys.* 2006;125(8):1-12. doi:10.1063/1.2222355
  15. Musia M of F, Barlett RJ (University of F. EOM-CCSDT study of the low-lying ionization potentials of ethylene, acetylene and formaldehyde. *Chem Phys Lett.* 2004;384:210-214.
  16. Oana CM, Krylov AI. Dyson orbitals for ionization from the ground and electronically excited states within equation-of-motion coupled-cluster formalism: Theory, implementation, and examples. *J Chem Phys.* 2007;127(23).  
doi:10.1063/1.2805393
  17. Frisch, M. J.; Trucks, G. W.; Schlegel, H. B.; Scuseria, G. E.; Robb, M. A.; Cheeseman, J. R.; Scalmani, G.; Barone, V.; Petersson, G. A.; Nakatsuji, H.; et al.. Gaussian 09, revision A.02; Gaussian, Inc.: Wallingford, CT, 2016.
  18. Shao, Y.; Molnar, L.; Jung, Y.; Kussman, J.; Ochsenfeld, C.; Brown, S.; Gilbert, A.; Slipchenko, L.; Levchenko, S.; O'Neill, D.; DiStasio, R. C., Jr. Advances in Methods and Algorithms in a Modern Quantum Chemistry Program Package. *Phys. Chem. Chem. Phys.* 2006, 8, 3172–3191.